Chemical Science

Cite this: DOI: 10.1039/c1sc00276g

www.rsc.org/chemicalscience

MINIREVIEW

Mechanochemistry of F_1 motor protein†‡

Hiroyuki Noji,*[a] Daichi Okuno[b] and Tomohiro Ikeda[a]

Received 7th May 2011, Accepted 20th June 2011
DOI: 10.1039/c1sc00276g

Although a variety of physical perturbations are utilised to control chemical reactions or bias chemical equilibria, mechanical force is not generally an option for controlling chemical reactions due to technical complexity. However, upon attaching handles to a responsive moiety and pulling, twisting or pushing it, unique means of controlling chemistry are permitted because mechanical force is intrinsically anisotropic for chemical structures. One remarkable example in natural systems is F_1-ATPase, the water-soluble part of F_oF_1-ATP synthase. F_1-ATPase is a rotary motor protein in which the rotor subunit rotates against the surrounding catalytic stator ring, hydrolysing ATP. A unique feature of F_1-ATPase is that it synthesises ATP against the large chemical potential of ATP hydrolysis when its rotation is mechanically reversed. This mini-review will introduce the latest findings about the mechanochemical properties of F_1-ATPase, and summarise the common concepts of mechanochemistry it shares with synthetic molecular systems.

Introduction: Molecular machines in cells

Living matter is dynamic; every cell moves and/or transforms its own shape actively and continuously. Even in apparently static cells, upon a closer look, one will observe that many intracellular structures are constantly moving and transforming. Although many motions do not exhibit clear directionality, implying that they are due to thermal agitation, many unidirectional motions or drastic structural changes are not attributable to thermal agitation. These dynamics are supported by molecular machines comprising proteins or RNA/protein conjugates. Myosin, kinesin, dynein and flagellar motor proteins are termed molecular motor proteins that exert force to support intracellular transportation or the large-scale transformation of cells or organelles, such as muscle fibre contraction, bacterial flagella rotation, and flagella beating in eukaryotic cells. In a limited sense, 'molecular motor' is the term used for proteins wherein their physiological roles are directly relevant to force generation. However, many proteins that were originally classified as enzymes have been reclassified as force-generating molecular machines. Prominent examples are enzymes involved in the central dogma of cell biology, such as DNA polymerase, RNA polymerase, and ribosome, whose principal physiological role is biopolymer production. A state-of-the-art single-molecule technique revealed that these molecules are also able to work against external forces to perform their functions.[1–6] In some cases, such non-molecular motor proteins generate much larger forces than do molecular motor proteins.[7,8] Thus, dynamics and force generation are common features of biology even at the molecular level.

Mechanochemical coupling of molecular machines

Most biomolecular machines consume adenosine triphosphate (ATP), hydrolysing it into adenosine diphosphate (ADP) and inorganic phosphate (P_i) as chemical fuel for functionality. Driven by the energy liberated by the ATP hydrolysis reaction, these proteins change their conformation and exert force. Unlike manmade combustion engines that convert chemical energy into mechanical work *via* air expansion, biomolecular machines directly convert energy derived from ATP hydrolysis into mechanical work. Thereby, they achieve high-energy conversion efficiency. Another remarkable feature of biomolecular machines that should be emphasised more, and will be a focus of this review, is that they can also convert energy in the reverse manner, *i.e.* they can modulate the chemical reaction equilibrium or rate constant upon external mechanical force input. One prominent example is F_oF_1-ATP synthase. This enzyme synthesises ATP against the large free energy of ATP hydrolysis (~48 kJ mol^{-1} under physiological conditions) upon mechanical manipulation by reverse rotation as discussed later in the text. In this review, we will focus on F_1-ATPase, the catalytic core of F_oF_1-ATP synthase, and provide a brief review about what we have learned about the mechanochemical coupling mechanism of F_1-ATPase mainly from single-molecule experiments using F_1-ATPase from

[a]*Department of Applied Chemistry, School of Engineering, The University of Tokyo, Bunkyo-ku, Tokyo, 113-8656, Japan. E-mail: hnoji@appchem.t.u-tokyo.ac.jp; Fax: +81-3-5841-1872; Tel: +81-3-5841-7252*
[b]*Laboratory for Cell Dynamics Observation, Quantitative Biology Center, RIKEN, 6-2-3 Furue-dai, Suita, Osaka 565-0874, Japan*
† Funding: This work was partially supported by Grants-in-Aid for Scientific Research (No. 18074005 to H. N.) and by special education and research expenses (to H. N.) from the Ministry of Education, Culture, Sports, Science, and Technology, Japan.
‡ Conflict of Interest: None declared.

thermophilic *Bacillus* PS3 (TF_1) whose mechanochemical properties are the best characterised among F_1-ATPases. For comparison, studies on another model system, F_1 from *Escherichia coli*, (EF_1) are also introduced arbitrarily.

F_oF_1-ATP synthase

F_oF_1-ATP synthase is found widely in the biological world, including in thylakoid membranes, the mitochondrial inner membrane, and the plasma membrane of bacteria. This enzyme synthesises ATP from ADP and P_i by using the electrochemical potential of protons across the membrane, *i.e.* it converts electrochemical potential into chemical energy. Under aerobic conditions, most ATP is synthesised by F_oF_1-ATP synthase. This enzyme also functions in the reverse direction when the electrochemical potential becomes insufficient; it catalyses proton pumping to generate electrochemical potential by hydrolysing ATP into ADP and P_i. F_oF_1-ATP synthase is a super-complex enzyme with a molecular weight of more than 500 kDa and consists of two rotary motors. One motor is F_1 (~380 kDa), which is the water-soluble part of ATP synthase. When isolated from the membrane portion, it acts as an ATP-driven motor; it rotates its inner subunit, resulting in ATP hydrolysis, and it is therefore termed F_1-ATPase. The other rotary motor of ATP synthase is F_o (~120 kDa), which is embedded in the membrane and generates rotary torque upon proton translocation that is driven by proton electrochemical potential (Fig. 1).[9] Bacterial F_1 is composed of $\alpha_3\beta_3\gamma\delta\varepsilon$ subunits. The minimum complex of F_1 as a motor is the $\alpha_3\beta_3\gamma$ subcomplex. The three α and three β subunits form the hexameric stator ring in which the α and β subunits are alternately arranged. The rotor shaft is the γ-subunit, which is accommodated in the central cavity of the $\alpha_3\beta_3$ ring. Upon ATP hydrolysis of the catalytic sites, F_1 rotates the γ subunit in the anticlockwise direction when viewed from the F_o side. The δ and ε subunits act as connectors between F_1 and F_o, each connecting the stator and rotor parts, respectively. F_o consists of ab_2c_{8-15} subunits. The number of c-subunits varies among species. The *c* subunits form the rotor ring complex by aligning in a circle. The c-ring and a-subunit form a proton pathway.[10] With the downhill proton flow through the proton channel, the c-ring rotates against the ab_2 subunits in the direction opposite that of the γ subunit of the F_1 motor.[11] Thus, in the F_oF_1 complex, F_o and F_1 push each other in the opposite direction. Under physiological conditions where the electrochemical potential of the protons is sufficiently large, F_o generates larger torque than does F_1 and then forcibly rotates the γ subunit in the clockwise direction. As a result, F_1 catalyses the reverse reaction, *i.e.* ATP synthesis, and this reaction is the principle physiological function of ATP synthase.

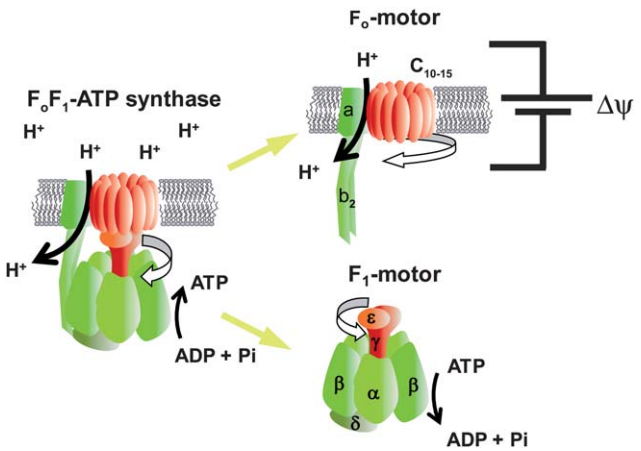

Fig. 1 F_o and F_1 motors of ATP synthase. Schematic images of F_oF_1-ATP synthase. The rotor and stator parts are shown in red and green, respectively. The subunit composition of F_1 and F_o are $\alpha_3\beta_3\gamma\delta\varepsilon$ and ab_2c_{10-15}, respectively. F_o is embedded in the cell membrane and rotates the c-ring against the ab_2 stator, which is driven by proton translocation down the proton electrochemical potential across the membrane. Isolated F_1 acts as the ATPase, and therefore, is referred to as F_1-ATPase. Hydrolysing ATP, F_1 rotates the γ subunit against the $\alpha_3\beta_3$-cylinder ring. In the full complex of F_oF_1, F_o exerts a larger torque, reverses the rotation of F_1, and leads to ATP synthesis from ADP and P_i.

F_1-ATPase

Catalytic reaction centres for ATP hydrolysis/synthesis reside at the three α–β interfaces, which are on the anticlockwise side of

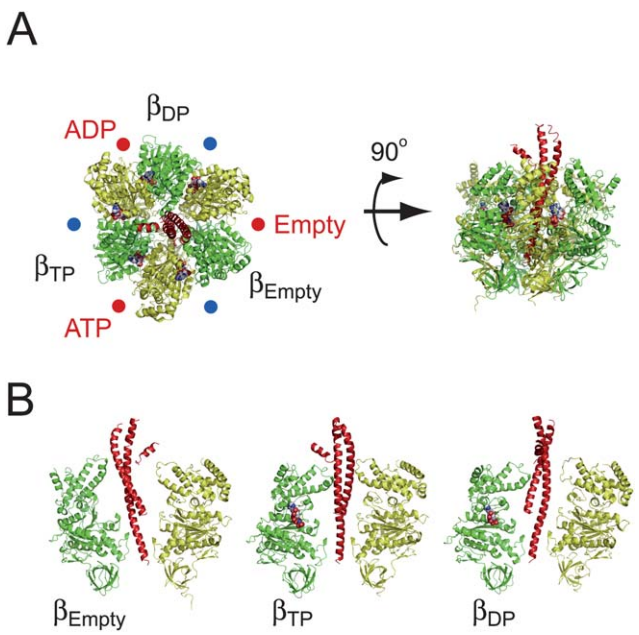

Fig. 2 Crystal structure of the $\alpha_3\beta_3\gamma$ subcomplex of F_1. The crystal structure of F_1 from bovine mitochondria (PDB code; 1BMF). The α, β and γ subunits are shown in yellow, green and red, respectively. (A) The left figure is viewed from the membrane side (F_o side), and is rotated 90° in the anticlockwise direction of the black arrow (right figure). The protruding part of γ is directed toward the F_o side. The catalytic sites are located at the α–β interface, and are indicated by red circles, primarily on the β subunit. Each site carries AMP-PNP, ADP, or is empty, and is designated as β_{TP}, β_{DP} or β_{empty}, respectively. The other interfaces are non-catalytic sites (blue circles), all of which are occupied with AMP-PNP. (B) Conformational states of the β subunit. Three α–β pairs with the γ subunit are shown. The α and β subunits are composed of the N-terminal domain, nucleotide-binding domain, and C-terminal domain (from bottom to top). β_{empty} has an open conformation in which the α-helical C-terminal domain rotates upwards to open the cleft of the nucleotide-binding pocket. Both β_{ATP} and β_{ADP} have a closed conformation entrapping the nucleotide within the closed pocket.

the β subunit as indicated with red circles in Fig. 2A. F_1 also has non-catalytic ATP-binding sites at the three α–β interfaces, but at the opposite side of β (blue circles in Fig. 2A). Whereas the catalytic site is formed mainly with amino acid residues from the β subunit, the non-catalytic sites are primarily located within the α subunit. The three catalytic sites on the β subunits work cooperatively during catalysis. The classic working model for F_1 is the 'binding change mechanism' proposed by Boyer.[12] One important feature of this model is that the affinity for nucleotides at each catalytic site is different from each other at any given time, and the statuses of the three β subunits cooperatively change in one direction accompanying γ rotation. This hypothesis is strongly supported by the X-ray crystallographic studies on bovine mitochondrial F_1 performed by Walker's group.[13] The first resolved crystal structure of F_1[13] revealed many essential structural features of F_1 at atomic resolution. Importantly, the catalytic β subunits differ from each other in conformation and in the catalytic state; one subunit binds to an ATP analogue, adenosine-5′-(β,γ-imino)triphosphate (AMP-PNP); the second binds to ADP; and the third is empty (Fig. 2A). Therefore, these sites are termed β_{TP}, β_{DP} and β_{empty}, respectively. Whereas β_{TP} and β_{DP} have a closed conformation wrapping bound nucleotides on the catalytic sites, β_{empty} has an open conformation swinging the C-terminal domain away from the binding site to open the cleft of the catalytic site (Fig. 2B). From these structural features, it is widely thought that the open-to-closed transition of the β subunits upon ATP binding pushes γ,[14] and the sequential conformational change among β subunits facilitates the unidirectional γ rotation, which was recently visualised in simultaneous imaging of the conformational change in the β subunit and γ rotation.[15] It should be mentioned that although the structural features found in the first crystal structure of F_1 were well conserved in the other crystal structures generated with different nucleotides or ligand analogues, there is a distinct exception[16]—when crystallised with a transition-state analogue complex ($ADP\text{-}AlF_4^-$), β_{empty} is also occupied with nucleotide, and adopts a half-closed conformation. This is assumed to represent a transition state before ADP release.

Single-molecule observation of F_1

Since the publication of the crystal structure, many studies have attempted to demonstrate the rotation of F_1. Crosslink exchange experiment between the β and γ subunits of EF_1[17] and the polarised absorption relaxation of F_1 from spinach chloroplasts[18] have proven the rotational motion of the γ subunit during catalysis. The unidirectional rotation of the γ subunit upon ATP hydrolysis was demonstrated with the direct observation of F_1 rotation under the microscope.[19] To suppress rotary Brownian motion, F_1 was immobilised on a glass surface modified with Ni-nitrilotriacetic acid (Ni-NTA) through the interaction between Ni-NTA and the His-tag, which was introduced at the N-terminus of the β subunit. In addition, a fluorescently labelled actin filament with a length of 0.6–4 μm and a diameter of 10 nm was attached to the γ subunit as the rotation marker to magnify the small motion of the γ subunit, whose radius is only 1 nm, which is much smaller than the spatial resolution (~200 nm) of a conventional microscope (Fig. 3A). Note that in recent studies, other types of probes such as polystyrene beads,

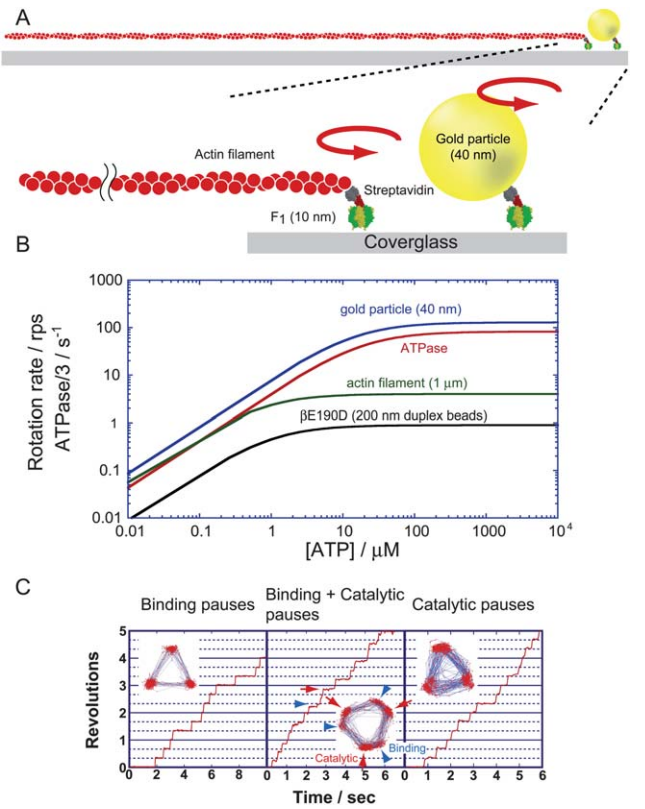

Fig. 3 Single-molecule rotation assay of F_1. (A) A schematic image of the experimental setup. The $\alpha_3\beta_3$ ring is fixed on the glass surface. A rotation probe, fluorescently labelled actin filament, or a gold particle is attached to the γ subunit to visualise the rotary motion under an optical microscope. (B) Rotational velocity *vs.* ATP concentration. Each line represents the experimentally obtained Michaelis–Menten curve for the rotation of wild-type F_1 visualised with 40-nm gold particles (blue)[28] and 1-μm actin filaments,[28] and for rotation of a mutant F_1 (βE190D) probed with 200-nm duplex beads (black)[30] whose hydrodynamic friction is comparable to that of the 1-μm actin filament. ATPase turnover rates determined in solution measurement that were corrected to equal the rotational rate by dividing by 3, are also shown (red).[28] To suppress the effect of the ADP-inhibited form, the solution contained lauryldimethylamine oxide, which relieves ADP inhibition. (C) Time courses of rotation and the trajectory of the centroid of the probe (insets). The left panel represents the rotation of the wild-type F_1 under ATP-limiting conditions (60 nM ATP). The middle panel shows the rotation of the mutant F_1-ATPase F_1 (βE190D), around the K_M region (2 μM ATP). The 120° step splits into 0 and 80° substeps, each intervened with a binding dwell and catalytic dwell, respectively. Arrowheads (blue) and arrows (red) indicate the positions of ATP binding and catalytic dwell, respectively. The right panel shows the rotation of F_1 (βE190D) at saturating ATP (2 mM). Rotation is paused at catalytic dwell.

gold colloidal beads, gold nanorods and magnetic beads have been used instead of actin filaments because the imaging of fluorescently labelled actin filaments suffers from photobleaching. Currently, this rotation assay is a simple and so established technique that even 8 years old children can execute this experiment. The rotational direction was always anticlockwise when viewed from the F_o side, and importantly, it was consistent with the expected rotary direction from the crystal structure. Assuming that the β subunit undergoes the conformational

transition from β_{empty} to β_{TP}, and then β_{DP}, each catalytic state must propagate in the anticlockwise direction, accompanying the anticlockwise γ rotation. The rotational velocity was far slower than the rate expected from bulk ATPase measurements because of the large hydrodynamic friction exerted on the rotating actin filament. However, this allows us to estimate the torque generated by individual F_1 molecules from the hydrodynamic friction in equilibrium with the torque of F_1. The torque was determined to be approximately 40 pN nm. Although this is a rough estimation without consideration of the viscosity increment in the immediate vicinity of glass surfaces, the value was recently confirmed to be valid using more precise torque measurements based on the fluctuation theorem, which estimates the entropy generation upon the rotation without assuming the friction coefficient.[20] Comparable or slightly higher torque values (33–50 pN nm) were reported for EF_1[21–24] and chloroplast F_1 (CF_1).[25] Among them, the estimation by Junge's group, 50 pN nm, would be more accurate because it was determined from the curvature of the rotating actin filament as the torque indicator to avoid the surface effect. Considering that the step size upon a single turnover of ATP hydrolysis is 120° as introduced in the following section, the work done by F_1 upon a single ATP hydrolysis is 80 pN nm or more, which essentially corresponds to the free energy released from the hydrolysis of a single ATP molecule under physiological conditions, suggesting 100% energy conversion efficiency for F_1.

Stepping rotation

Many attempts have been made to resolve rotary motion into discrete steps to clarify how the rotation is coupled with each elementary catalytic step of ATP hydrolysis: ATP binding, hydrolysis and the release of ADP and P_i. The stepping rotation was first observed in the rotation assay with actin filaments under ATP-limiting conditions, where the ATP-binding process limits the overall turnover rate of the catalysis. When [ATP] is well below the Michaelis–Menten constant (K_M) of the rotation (~1 μM), F_1 displayed discrete 120° steps, each intervened with pauses as expected from the pseudo-three-fold symmetry of the $\alpha_3\beta_3$-ring (Fig. 3B and C). The mean dwell time of the pause was inversely proportional to [ATP], suggesting that the single ATP-binding event triggers individual 120° steps.[26] The coupling ratio of a single 120° step per ATP was directly confirmed in a later study.[27] Under ATP-saturating conditions, the stepping nature of F_1 rotation was undetectable due to the damping effect of high viscous friction against the rotating actin filament. When 40-nm gold colloid, which is comparable in size to F_1, was employed as the probe, the temporal resolution was largely improved so that 120° steps terminated by a 2-ms pause were observed even in saturating conditions. Later, the pause was revealed to be the waiting state for hydrolysis and P_i release (see below). The rotational velocity reached the maximum rate, which is determined not by mechanical rotation but by catalytic reaction. The observed rate slightly exceeded the expected rate from ATP hydrolysis activity measured in bulk solution.[28] The discrepancy in the rates is attributed to some fraction of F_1 being in an inactive state, the so-called ADP-inhibited form,[29] in the ensemble solution measurement. Near the K_M, where time constants for the ATP-binding step and catalysis are comparable, the rotation was further resolved into 90 and 30° substeps,[28] which were later revised to be 80 and 40° substeps.[30] The dwell time before the 80° substep is [ATP]-dependent, and therefore, ATP binding was identified as a trigger reaction of the 80° substep. When the catalytically critical glutamic acid termed the 'general base' (βE190 inTF_1) was substituted with aspartic acid, the time constant of pause before the 40° substep was significantly slowed, implying that the 40° substep is triggered by ATP hydrolysis. The time constant of hydrolysis on the mutant F_1 is 300 ms. The long pause permits observation of the stepping motion even using large probes such as 200-nm plastic beads (Fig. 3B and C). Near K_M, the mutant F_1 displays clear 80 and 40° substeps (Fig. 3C). Recent elaborated kinetic analyses of the substeps revealed that the 80° substep is triggered by ATP binding and ADP release, whereas the 40° substep is triggered by ATP hydrolysis and P_i release.[28,30,31] The angular dwelling positions before the 80 and 40° substeps are termed the binding angle and catalytic angle (Fig. 3C), respectively. For EF_1 rotation, although 120° stepping rotation was detected, clear 80 and 40° substeps have not been reported.[24,32] This would be at least partially due to the more compliant γ shaft of EF_1,[33] which obscures the dwelling state between substeps.

Reaction scheme

All of the elementary reaction steps were found to occur at the binding or catalytic angle. However, because there are three positions for the binding and catalytic angles during a turn, determining the angle at which each reaction occurs is required to establish the complete reaction scheme. The angle for hydrolysis was determined using a hybrid F_1 carrying a single copy of the aforementioned mutant β subunit βE190D.[34] This hybrid enables the identification of the hydrolysis angle because the incorporated mutant β subunit exhibits distinctly long pauses at two positions: one pause occurs at the ATP-binding angle of the mutant β subunit (0°), and the other occurs at +200° from the binding angle. Thus, the hydrolysis angle was determined to be 200°. Simultaneous imaging of fluorescently labelled ATP and γ rotation revealed that ADP release occurs at 240°.[31,35] The timing of P_i release has recently been determined to be at 320° in another type of experiment[36] where F_1 was stalled with magnetic tweezers during hydrolysis dwell. On the basis of the observation that bound ATP undergoes hydrolysis and synthesis in a reversible manner, it was revealed that P_i (or thiophosphate) is not released immediately after hydrolysis at 200°. Because P_i release has to occur after hydrolysis and at a catalytic angle, it was concluded that P_i release occurs at 320°. Thus, the present reaction scheme of rotation and catalysis was established as follows: ATP binding at 0°, hydrolysis at 200°, ADP release at 240°, and P_i release at 320° (Fig. 4). In this reaction scheme, the average occupancy of the catalytic sites with nucleotide is around two. On the other hand, biochemical measurements on nucleotide titration suggest the catalytic sites are fully filled with nucleotides. The explanation on the apparent discrepancy is that the catalytic site of 320° state can bind to ATP under ATP-saturating condition. It should be mentioned that there is a controversy about the timing of P_i release. Several groups proposed that P_i is released at 200° immediately after hydrolysis due to the simplicity, or based on

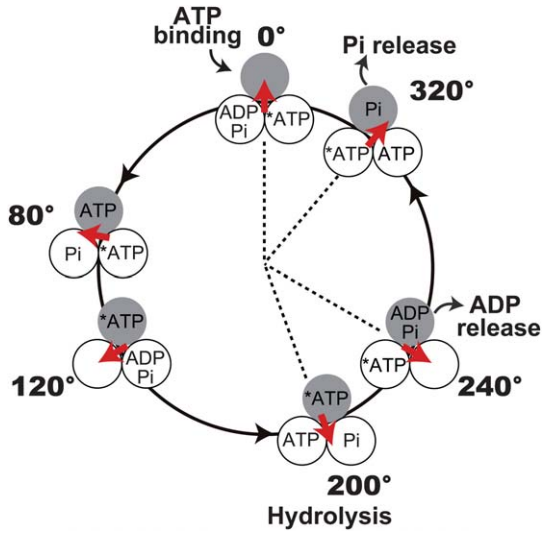

Fig. 4 Mechanochemical coupling scheme of F_1. Each circle represents the chemical state of the catalytic sites on the β subunit. 0° is defined as the ATP-binding angle for the catalytic site represented as the gray circle. At 200°, the catalytic site hydrolyses ATP into ADP and P_i, which are released at 240 and 320°, respectively. Other catalytic sites also obey the same reaction scheme, and the reaction phase is different from the gray one by ±120°. Another model for P_i release is also proposed (see text). At ATP-saturating conditions, the catalytic site of 320° state can bind to ATP, and thus the occupancy of catalytic sites with nucleotide reaches 3.

the biochemical titrations of catalytic site occupancy with a nucleotide.[37,38]

ATP synthesis upon reverse rotation

The essential properties and basic mechanochemical coupling scheme of F_1 as an ATP-driven motor have been nearly established. However, the physiological role of F_oF_1-ATP synthase, *i.e.* ATP synthesis, has not been sufficiently studied in single-molecule experiments. If ATP synthesis is a simple reverse reaction of hydrolysis, forcibly reversing the rotation of F_1 should lead to efficient ATP synthesis. To verify this hypothesis, two lines of experiments have been performed. In the first type of experiment,[39] a large number of F_1 molecules were enclosed in an observation chamber and forcibly rotated in the reverse direction with a magnetic tweezer system. The synthesised ATP was detected as bioluminescence using the luciferin–luciferase system. Although ATP synthesis upon reverse rotation was clearly demonstrated, the uncertainty of the number of active F_1 molecules in the chamber did not allow quantitative estimation of the mechanochemical coupling ratio. Therefore, the following experiment focused on a single active F_1 molecule to determine the coupling ratio.[27] The technical issue to be addressed was the detection of a very small number of ATP molecules generated from a single F_1 molecule. Even if we assume that F_1 synthesises three ATP molecules per revolution at 10 Hz for 1 min, the total number of ATP molecule is only 1800 molecules (3.0×10^{-21} mole), which is far below the detection limit of the luciferase assay. To address this issue, a microscopic reaction chamber system was developed using a microfabrication technique. The developed system has identically shaped reaction chambers, each of which is a few microns in scale and has a volume of 6 fL.[40] Because the extremely small reaction volume results in high concentration, it is possible to detect the small amount of reaction product yielded from a single enzyme molecule. A single F_1 molecule was encapsulated in a micro-chamber (Fig. 5A and B). After forcible reverse rotation with magnetic tweezers, F_1 was released from the tweezers. Because

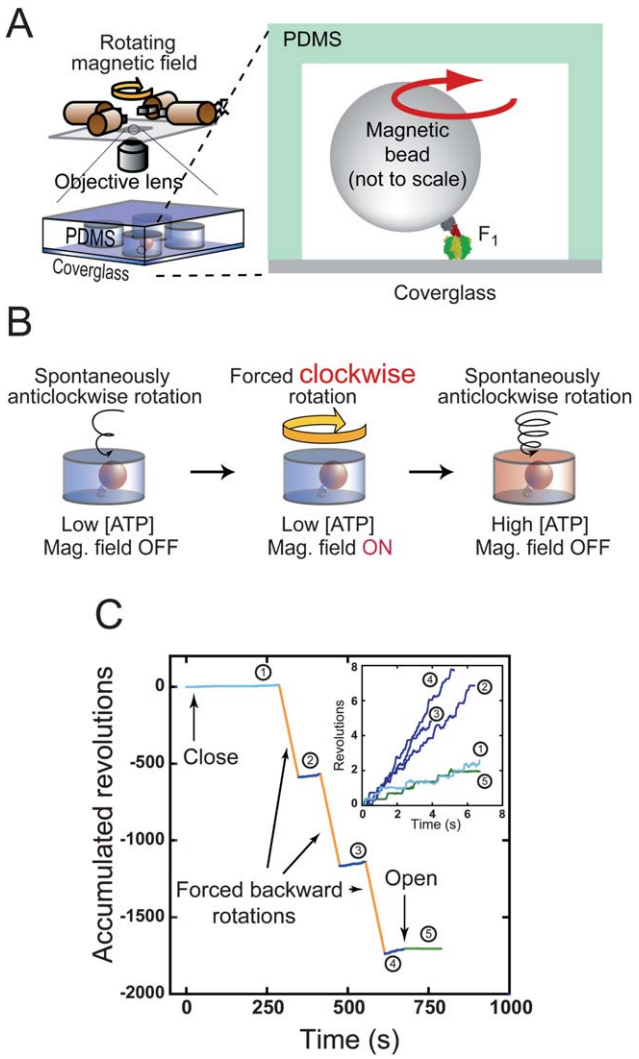

Fig. 5 ATP synthesis upon reverse rotation of F_1. (A) Schematic drawing of experimental setup. (B) Experimental procedure of ATP synthesis. Active single F_1 is enclosed in a micron-sized reaction chamber (left). A magnetic bead attached to the γ subunit is forcibly rotated by magnetic tweezers (centre). Newly synthesised ATP is accumulated in the chamber. The number of synthesised ATP molecules is determined from the increments in the ATP-driven rotational speed of released F_1 (right). (C) Time courses of the ATP synthesis experiment. A typical data set is shown. After entrapping, the rotational velocity under the initial condition was recorded (1), and then a rotating magnetic field was applied. After forcible rotation, F_1 was released to record the velocity (2). This procedure was repeated (3, 4), and was terminated by opening the chamber to confirm that F_1 resumed its original velocity (5). Insets show the closed-up time course of spontaneous rotation. Velocity increment shows the ATP synthesis during forced backward rotation (orange lines).

the rotational rate of ATP-driven rotation is proportional to [ATP] under the experimental conditions, one can measure the increment of [ATP] as that of the ATP-driven rotation rate (Fig. 5C). It was found that F_1 undergoes highly efficient ATP synthesis of ~80% (2.3 ATP molecules per turn). The high reversibility of mechanochemical coupling is the remarkable feature of F_1 that distinguishes it from other molecular motors; other motor proteins such as kinesin and myosin do not synthesise ATP when the movements are reversed by external force. Single-molecule manipulation for the elucidation of mechanochemical properties has not been attempted for EF_1, although optical tweezers were developed for the manipulation.[41] Therefore, in the following sections as well as this section, all of the introduced works describe TF_1.

ATP binding enhanced by forcible forward rotation

The aforementioned finding that the reverse rotation leads to the reverse chemical reaction is conceptually simple, and is the expected result for the verification of F_1 rotation. However, the chemical equilibrium of ATP hydrolysis/synthesis is significantly inclined to hydrolysis by a factor of 1×10^8 without external perturbation. Furthermore, proteins have a large number of degrees of freedom in their conformations. Considering these facts, it is fascinating that only by manipulating the sole degree of freedom of F_1, the rotary angle of the γ subunit, one can synthesise ATP against the large chemical potential of ATP hydrolysis. There is no other catalyst exhibiting such a feature in natural systems or manmade catalysts. To achieve highly efficient mechanochemical coupling, individual catalytic steps—ATP-binding, hydrolysis and product release—should be tightly coupled with γ rotation in F_1. In other words, these reactions should be modulated upon γ rotation. To elucidate the mechanical modulation of the ATP-binding process, the microchamber system was again used.[42] In this experiment, the F_1 molecule was enclosed in a similar chamber as used for the ATP synthesis experiment. However, the molecules were rotated in the 'forward' direction. Only a limiting amount of ATP was added to the solution to monitor ATP consumption as the decrement in the velocity of spontaneous rotation. Because only the ATP-binding step has a long time constant compared with other reaction steps under this experimental condition, the efficiency of ATP binding during forcible rotation was determined as the net coupling efficiency. After each forcible rotation, F_1 resumed its spontaneous rotation and its velocity decreased, suggesting that the forcible rotation is well coupled with ATP hydrolysis. Surprisingly, even while rotating at a much faster rate than that of spontaneous rotation, F_1 still couples the rotation with hydrolysis. This implies that the mechanical forward rotation largely enhances the ATP-binding rate. Numerical analysis of this result suggests that the rate constant of ATP binding increases significantly, at least by a factor of 10 during the 80° substep.

Additional evidence for mechanical modulation of the reaction

Another implication regarding the mechanical modulation of catalysis came from the manipulation of F_1 in an inhibitory state. During catalytic turnover in ATP hydrolysis, F_1 stochastically lapses into an inhibitory state, pausing rotation by tightly holding ADP that has to be released to continue the reaction.[29,43] This inhibitory state is termed the ADP-inhibited form. When mechanically manipulated, F_1 readily resumes the active rotation, releasing the tightly bound ADP into solution.[44] This mechanical activation highly depends on the direction of manipulation and duration of manipulation; when rotated in the forward direction and held for a longer time, the activation probability drastically increases. It was demonstrated that the rate constant of mechanical activation triggered by ADP release increases exponentially. Recently, we performed similar experiments to investigate how ATP binding and hydrolysis are modulated upon γ rotation by stalling F_1 in the ATP-binding or hydrolysis-waiting state.[45] It was found that the ATP-binding rate and association constant of ATP are also exponentially enhanced upon γ rotation (by a factor of 1×10^4 or more for the association constant during the 80° substep), but hydrolysis exhibits weak angle dependence. These findings indicate that the ATP-binding process is the major torque-generating step. All of the reaction steps examined thus far are accelerated upon γ subunit rotation. Since these reactions occur on different β subunits, each β subunit accelerates other reactions on different β subunits by pushing the γ subunit. This would be one of the principal bases of cooperativity among β subunits. Although ATP synthesis *via* the reverse rotation is a unique feature of F_1, the core structural element around the catalytic site of F_1 shares common and well-conserved structural features with other ATP-driven motors and ATPases.[46] Considering this point, the ability to mechanically modulate catalysis would be shared by other molecular machines, although the degree of sophistication of mechanochemical coupling would be largely different. In fact, several reports demonstrated that the catalytic reaction rate of myosin or kinesin motor could be enhanced or suppressed by external manipulation.[47–50] These properties are discussed in the context of cooperativity between the 2 catalytic head domains of the motors.

Implications for synthetic molecular systems

The important implications we learned from F_1-ATPase are as follows. (1) Mechanical force can regulate and modulate the rate and equilibrium constants of chemical reactions; (2) mechanical modulation enables programming of cooperativity among catalytic reaction centres and leads to the unidirectional motion of molecular machines; and (3) the mechanical connection of two motors allows novel energy conversion. The same concepts should be applicable to synthetic chemical molecules. Although this has not been attempted frequently, the mechanical control of chemical reactions has been reported. Moore and co-workers successfully demonstrated mechanochemistry in synthetic molecules by using a polymeric gel.[51] Tensile force on the polymer gel induced the structural isomerisation of a mechanophore moiety introduced in the polymer chain. Similar attempts were made using a different method;[52,53] a responsive moiety was linked to polymer chains, and the solution of the conjugate was subjected to an ultrasonic wave that stretched the polymer and thus exerted tensile force on the moiety. Moore's group reported that a geometrically specific reaction of a cyclobutene ring opening

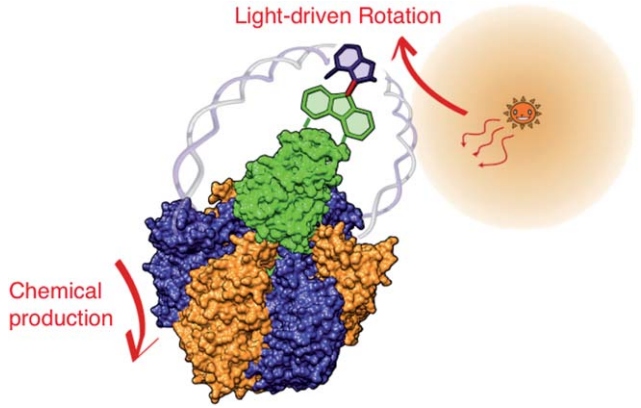

Fig. 6 Light-driven ATP synthesis by combination of light-driven artificial motor and F_1-ATPase. Schematic image of the artificial hybrid system composed of two different motors: synthetic light-driven motor and F_1-ATPase. Rotor parts are directly linked, and stator parts are connected *via* a flexible joint (DNA strand). The chemical structure of the synthetic motor does not show the reality. The expectation is that the light-driven motor functions similarly as F_o in ATP synthase to reverse F_1 and induce ATP synthesis.

was induced under tensile force.[53] Initiation of the catalytic reaction[52] by ultrasonically induced stretching was also demonstrated by the Sijbesma group.[52] Once the state-of-the-art single-molecular manipulation and analysis are applied to such synthetic molecular systems, new experimental approaches for more quantitative and precise control of mechanophores will be enabled, leading to the rational design of mechanosensitive moieties or molecular systems.

There are also reports on the development of unidirectionally moving synthetic molecular motors[54] such as the overcrowded alkenes developed by Feringa[55] and the multistation catenanes and molecular walkers developed by Leigh.[56,57] We are very interested in these works. However, although their chemical properties were extensively studied, the mechanical properties of synthetic motors such as torque or force and step size remain to be elaborated. In addition, to our knowledge, the mechanical linkage of two molecular motors for energy conversion as observed in F_oF_1-ATP synthase has not yet been conducted. We do not consider this a fancy technique. Rather, it appears feasible to connect existing motors, for example, F_1-ATPase and a light-driven synthetic motor[54] (Fig. 6). When linked with consideration of the step size and the torque of two motors, the hybrid motor realises the photosynthesis that directly converts light energy into chemical energy *via* ATP synthesis. The assembly of biomolecular and synthetic molecular motors would pave the way for new energy conversion technologies.

Acknowledgements

We thank all members of the Noji Laboratory.

References

1 A. Goel, M. D. Frank-Kamenetskii, T. Ellenberger and D. Herschbach, *Proc. Natl. Acad. Sci. U. S. A.*, 2001, **98**, 8485–8489.
2 B. Maier, D. Bensimon and V. Croquette, *Proc. Natl. Acad. Sci. U. S. A.*, 2000, **97**, 12002–12007.
3 G. J. Wuite, S. B. Smith, M. Young, D. Keller and C. Bustamante, *Nature*, 2000, **404**, 103–106.
4 R. V. Dalal, M. H. Larson, K. C. Neuman, J. Gelles, R. Landick and S. M. Block, *Mol. Cell*, 2006, **23**, 231–239.
5 M. H. Larson, W. J. Greenleaf, R. Landick and S. M. Block, *Cell*, 2008, **132**, 971–982.
6 M. D. Wang, M. J. Schnitzer, H. Yin, R. Landick, J. Gelles and S. M. Block, *Science*, 1998, **282**, 902–907.
7 Y. R. Chemla, K. Aathavan, J. Michaelis, S. Grimes, P. J. Jardine, D. L. Anderson and C. Bustamante, *Cell*, 2005, **122**, 683–692.
8 D. E. Smith, S. J. Tans, S. B. Smith, S. Grimes, D. L. Anderson and C. Bustamante, *Nature*, 2001, **413**, 748–752.
9 M. Yoshida, E. Muneyuki and T. Hisabori, *Nat. Rev. Mol. Cell Biol.*, 2001, **2**, 669–677.
10 W. Junge, H. Lill and S. Engelbrecht, *Trends Biochem. Sci.*, 1997, **22**, 420–423.
11 M. Diez, B. Zimmermann, M. Borsch, M. Konig, E. Schweinberger, S. Steigmiller, R. Reuter, S. Felekyan, V. Kudryavtsev, C. A. Seidel and P. Graber, *Nat. Struct. Mol. Biol.*, 2004, **11**, 135–141.
12 P. D. Boyer, *Annu. Rev. Biochem.*, 1997, **66**, 717–749.
13 J. P. Abrahams, A. G. Leslie, R. Lutter and J. E. Walker, *Nature*, 1994, **370**, 621–628.
14 G. Oster and H. Wang, *J. Bioenerg. Biomembr.*, 2000, **32**, 459–469.
15 T. Masaike, F. Koyama-Horibe, K. Oiwa, M. Yoshida and T. Nishizaka, *Nat. Struct. Mol. Biol.*, 2008, **15**, 1326–1333.
16 R. I. Menz, J. E. Walker and A. G. Leslie, *Cell*, 2001, **106**, 331–341.
17 T. M. Duncan, V. V. Bulygin, Y. Zhou, M. L. Hutcheon and R. L. Cross, *Proc. Natl. Acad. Sci. U. S. A.*, 1995, **92**, 10964–10968.
18 D. Sabbert, S. Engelbrecht and W. Junge, *Nature*, 1996, **381**, 623–625.
19 H. Noji, R. Yasuda, M. Yoshida and K. Kinosita, Jr., *Nature*, 1997, **386**, 299–302.
20 K. Hayashi, H. Ueno, R. Iino and H. Noji, *Phys. Rev. Lett.*, 2010, **104**, 218103.
21 H. Noji, K. Hasler, W. Junge, K. Kinosita, Jr., M. Yoshida and S. Engelbrecht, *Biochem. Biophys. Res. Commun.*, 1999, **260**, 597–599.
22 H. Omote, N. Sambonmatsu, K. Saito, Y. Sambongi, A. Iwamoto-Kihara, T. Yanagida, Y. Wada and M. Futai, *Proc. Natl. Acad. Sci. U. S. A.*, 1999, **96**, 7780–7784.
23 O. Panke, D. A. Cherepanov, K. Gumbiowski, S. Engelbrecht and W. Junge, *Biophys. J.*, 2001, **81**, 1220–1233.
24 D. Spetzler, J. York, D. Daniel, R. Fromme, D. Lowry and W. Frasch, *Biochemistry*, 2006, **45**, 3117–3124.
25 T. Hisabori, A. Kondoh and M. Yoshida, *FEBS Lett.*, 1999, **463**, 35–38.
26 R. Yasuda, H. Noji, K. Kinosita, Jr. and M. Yoshida, *Cell*, 1998, **93**, 1117–1124.
27 Y. Rondelez, G. Tresset, T. Nakashima, Y. Kato-Yamada, H. Fujita, S. Takeuchi and H. Noji, *Nature*, 2005, **433**, 773–777.
28 R. Yasuda, H. Noji, M. Yoshida, K. Kinosita, Jr. and H. Itoh, *Nature*, 2001, **410**, 898–904.
29 Y. Hirono-Hara, H. Noji, M. Nishiura, E. Muneyuki, K. Y. Hara, R. Yasuda, K. Kinosita, Jr. and M. Yoshida, *Proc. Natl. Acad. Sci. U. S. A.*, 2001, **98**, 13649–13654.
30 K. Shimabukuro, R. Yasuda, E. Muneyuki, K. Y. Hara, K. Kinosita, Jr. and M. Yoshida, *Proc. Natl. Acad. Sci. U. S. A.*, 2003, **100**, 14731–14736.
31 K. Adachi, K. Oiwa, T. Nishizaka, S. Furuike, H. Noji, H. Itoh, M. Yoshida and K. Kinosita, Jr., *Cell*, 2007, **130**, 309–321.
32 B. Zimmermann, M. Diez, N. Zarrabi, P. Graber and M. Borsch, *EMBO J.*, 2005, **24**, 2053–2063.
33 H. Sielaff, H. Rennekamp, S. Engelbrecht and W. Junge, *Biophys. J.*, 2008, **95**, 4979–4987.
34 T. Ariga, *BioSystems*, 2008, **93**, 68–77.
35 T. Nishizaka, K. Oiwa, H. Noji, S. Kimura, E. Muneyuki, M. Yoshida and K. Kinosita, Jr., *Nat. Struct. Mol. Biol.*, 2004, **11**, 142–148.
36 R. Watanabe, R. Iino and H. Noji, *Nat. Chem. Biol.*, 2010, **6**, 814–820.
37 W. Junge, H. Sielaff and S. Engelbrecht, *Nature*, 2009, **459**, 364–370.
38 R. Shimo-Kon, E. Muneyuki, H. Sakai, K. Adachi, M. Yoshida and K. Kinosita, Jr., *Biophys. J.*, 2010, **98**, 1227–1236.
39 H. Itoh, A. Takahashi, K. Adachi, H. Noji, R. Yasuda, M. Yoshida and K. Kinosita, *Nature*, 2004, **427**, 465–468.
40 Y. Rondelez, G. Tresset, K. V. Tabata, H. Arata, H. Fujita, S. Takeuchi and H. Noji, *Nat. Biotechnol.*, 2005, **23**, 361–365.

41 T. Pilizota, T. Bilyard, F. Bai, M. Futai, H. Hosokawa and R. M. Berry, *Biophys. J.*, 2007, **93**, 264–275.
42 Y. Iko, K. V. Tabata, S. Sakakihara, T. Nakashima and H. Noji, *FEBS Lett.*, 2009, **583**, 3187–3191.
43 J. M. Jault, C. Dou, N. B. Grodsky, T. Matsui, M. Yoshida and W. S. Allison, *J. Biol. Chem.*, 1996, **271**, 28818–28824.
44 Y. Hirono-Hara, K. Ishizuka, K. Kinosita, Jr., M. Yoshida and H. Noji, *Proc. Natl. Acad. Sci. U. S. A.*, 2005, **102**, 4288–4293.
45 R. Watanabe and D. Okuno *et al.*, to be submitted.
46 H. Noji, T. Amano and M. Yoshida, *J. Bioenerg. Biomembr.*, 1996, **28**, 451–457.
47 Y. Oguchi, S. V. Mikhailenko, T. Ohki, A. O. Olivares, E. M. De La Cruz and S. Ishiwata, *Proc. Natl. Acad. Sci. U. S. A.*, 2008, **105**, 7714–7719.
48 Y. Oguchi, S. V. Mikhailenko, T. Ohki, A. O. Olivares, E. M. De La Cruz and S. Ishiwata, *Nat. Chem. Biol.*, 2010, **6**, 300–305.
49 S. Uemura and S. Ishiwata, *Nat. Struct. Biol.*, 2003, **10**, 308–311.
50 S. Uemura, K. Kawaguchi, J. Yajima, M. Edamatsu, Y. Y. Toyoshima and S. Ishiwata, *Proc. Natl. Acad. Sci. U. S. A.*, 2002, **99**, 5977–5981.
51 D. A. Davis, A. Hamilton, J. Yang, L. D. Cremar, D. Van Gough, S. L. Potisek, M. T. Ong, P. V. Braun, T. J. Martinez, S. R. White, J. S. Moore and N. R. Sottos, *Nature*, 2009, **459**, 68–72.
52 A. Piermattei, S. Karthikeyan and R. P. Sijbesma, *Nat. Chem.*, 2009, **1**, 133–137.
53 C. R. Hickenboth, J. S. Moore, S. R. White, N. R. Sottos, J. Baudry and S. R. Wilson, *Nature*, 2007, **446**, 423–427.
54 E. R. Kay, D. A. Leigh and F. Zerbetto, *Angew. Chem., Int. Ed.*, 2007, **46**, 72–191.
55 N. Koumura, R. W. Zijlstra, R. A. van Delden, N. Harada and B. L. Feringa, *Nature*, 1999, **401**, 152–155.
56 D. A. Leigh, J. K. Wong, F. Dehez and F. Zerbetto, *Nature*, 2003, **424**, 174–179.
57 M. von Delius, E. M. Geertsema and D. A. Leigh, *Nat. Chem.*, 2009, **2**, 96–101.

